Desalination and Water Treatment
www.deswater.com
doi: 10.1080/19443994.2015.1010236

57 (2016) 6540–6553
March

Taylor & Francis
Taylor & Francis Group

Simultaneous adsorption of lead (II) and 3,7-Bis(dimethylamino)-phenothiazin-5-ium chloride from aqueous solution by activated carbon prepared from plantain peels

Edu I. Inam[a,*], Ubong J. Etim[b], Ememobong G. Akpabio[a], Saviour A. Umoren[a]

[a]*Faculty of Science, Department of Chemistry, University of Uyo, Akwaibom State, Nigeria, Tel. +234 8181750861; emails: eduinam@uniuyo.edu.ng (E.I. Inam), ememaka4life@yahoo.com (E.G. Akpabio), Tel. +966138607902; email: saviourumoen@yahoo.com (S.A. Umoren)*
[b]*State Key Laboratory of Heavy Oil Processing, School of Science, China University of Petroleum, Huadong, 266280, Qingdao, P.R. China, Tel. +86 18254282115; email: uje4sure2010@yahoo.com*

Received 9 November 2014; Accepted 2 January 2015

ABSTRACT

Activated carbon has been prepared from plantain peels unripe, a biowaste from confectioneries for investigation of its adsorption efficiency in binary system of lead (II) and 3,7-Bis (dimethylamino)-phenothiazin-5-ium chloride as common water pollutants. The prepared carbons were characterized using nitrogen adsorption, FTIR spectroscopy, and XRD. Batch adsorption experiments were conducted to determine most probable conditions of adsorption maximum via varying adsorbent concentration, initial pollutants concentration, and pH of adsorption. Adsorption was found to be dependent on the factors studied. Favorable adsorption was recorded at initial concentration of 300 mg/dm^3 after 30 min. Equilibrium and kinetic data were modeled using well-known isotherm and kinetic models. Results deviated largely from Langmuir monolayer, Freundlich multilayer and extended Langmuir isotherm models suggesting a mutual interaction of the adsorbates in solution which is shown with data obtained from competitive adsorption evaluation. Kinetics was fast and data fitted extensively to pseudo-second-order kinetic model with good correlation coefficient greater than 0.99. From the results of the analysis, mechanism of adsorption is proposed and adsorption using this adsorbent is feasible and could be developed as a low-cost alternative for the treatment of industrial effluent system of dye-metal matrix.

Keywords: Adsorption; Plantain peel; Wastewater; Dye; Lead

1. Introduction

Often surface run-offs get contaminated by industrial discharges. A number of industries including textile, battery, paint, and metallurgy are good culprits in this direction. This, therefore, presents a considerable challenge to industrialist as regards proper waste disposal and management. For example, real textile wastewater is a complex mixture of many pollutants including acids, dispersants, alkalis, dyes, heavy metals, organic-chlorines, phthalates, pigments, pharmaceuticals, and salts [1,2]. The presence of even low levels of lead and dyes in water is a concern because it tends to bioaccumulate in the food chain [3]. Waste

*Corresponding author.

streams generated from textile industries are hazardous to the environment and difficult to biodegrade owing to the presence of these chemicals [4]. These affect physio-chemical properties of water altering the pH, and increasing biochemical oxygen demand and chemical oxygen demand levels. Though many components of textile wastewater can be decomposed and prevented from entering our waterways, it is impossible to completely eliminate all pollutants created during the different stages of textile manufacturing processes. Several methods of water treatment including wastewaters have been reported which include electrocoagulation [5], electrochemical method [6], sedimentation, filtration, flocculation, oxidation, and adsorption [7]. Amongst the said methods, adsorption has been widely applied for wastewater treatment. Adsorption has the ability to remove stubborn contaminants from solution which is difficult to breakdown by known biological processes [7]. Many adsorbents such as alumina, silica gel, zeolites, chitosan bead, and activated carbons [7–9] have been known for their good adsorption capacities for pollutant removal applications. But some of these adsorbents such as silica gels, aluminas, and zeolites suffer lack of applications relating to cost implications and competitiveness in other applications including catalyst. This necessitates search for substitutes which will not only check cost of procurement but also ease of application, reuse, and flexibility. Toward this end, activated carbons from biomass have been widely utilized. The adsorption effectiveness and commercial applicability of activated carbon are well known. Although commercial activated carbon is expensive [2,10,11], relatively cheap and high-performance carbons with similar functionalities can be prepared from agricultural waste and biomass [10,12,13]. Agricultural wastes and residues offer highly economical, biodegradable, and renewable sources of activated carbon. They are inexpensive and abundantly available, and consist mainly of cellulose, hemicelluloses, and lignin [14], possessing excellent qualities as adsorbents for many types of pollutants owning to the presence of some functional groups such as hydroxyl, carboxyl, phenols, and carbonyl on the surface that takes part in binding with the pollutants [15].

Activated carbon prepared from agricultural wastes such as orange, bean, garlic, pomegranate peels, coconut husk, bagasse, kolanut shell just to mention but a few and their application in adsorption of dyes have been reported in the literature by some researchers [16–21]. However, most of the adsorption studies were carried out in solutions of single component (dye or metal ions). Reports on comparative studies on simultaneous adsorption of binary components (dye and metal ions) including low-cost adsorbents are very scanty [22–30]. For instance, Visa et al. [22] studied the effect of methylene blue (MB) adsorbed on the surface of fly ash on the removal efficiency of Cd (II), Cu (II), and Ni (II) ionic species from complex, multi-cationic dye solutions. This study showed that high removal performances were recorded at low heavy metal concentration while the uptake of these metals was affected by competitive adsorption processes as their concentrations increased. In a similar study, adsorption of copper, nickel, and zinc on dye loaded groundnut shells and sawdust from aqueous solutions was reported by Shukla and Pai [23]. The authors showed that application of the dye to these materials resulted in an enhancement of adsorption capacities for heavy metals. Tovar-Gomez et al. [24] in their study using activated carbon revealed both antagonistic and synergistic effects on adsorption in ternary solutions of heavy metals and dye. Dye-enhanced removal of metals species and reduced the competitive adsorption between the metal ions present in some of the multicomponents solutions. Hernandez-Montoya et al. [25] reported antagonistic effects on adsorption of heavy metals Pb (II), Ni (II), and Zn (II), and acid blue 25, basic blue 9, and basic violet 3 dye-metal systems using zeolite. Their results revealed adsorption of basic blue dye was greatly reduced in the presence of heavy metals. Gong et al. [26] studied continuous adsorption of Pb (II) and MB on graphene oxide (GO) using a fixed-bed column. Their results showed that removal of MB was enhanced in the presence of Pb (II). The authors explained high adsorption of MB in the mixed solution was caused by p–p interaction between MB and GO on the surface of the adsorbent. In a similar study by Ding et al. [27] using chemically modified biomass, the authors reported simultaneous adsorption of both Pb (II) and MB, with Pb (II) preferentially adsorbed at higher Pb (II) to MB molar ratio, but the Pb (II) adsorbed at equilibrium decreased with increasing preloading of MB, suggesting competitive sorption of the two contaminants in solution. Deng et al. [28] in their report of cooperate removal of Cd (II) and ionic dyes, orange green (OG) and MB from aqueous solution using magnetic graphene oxide (MGO) nanocomposites as adsorbent observed synergic adsorption of OG in Cd (II)-OG binary system against a suppressed effect of Cd (II) removal in Cd (II)-MB system. Others synergic metal-dye systems have been reported [29,30]. In this study, we present the application of activated carbon from plantain peels for the treatment of a supposed binary system of dye and heavy metal (textile wastewater). Plantain peels may be regarded as the outer layer of the plantain fruit normally discarded as waste during its preparation for food. We also report

the interaction of the pollutants coexisting on extraction performance of the prepared carbon through equilibrium isotherm.

2. Materials and methods

2.1. Materials

All chemical reagents including H_2SO_4, NaOH, HCl, and 3,7-Bis(dimethylamino)-phenothiazin-5-ium chloride (Sigma Aldrich) were of analytical grade and were used without further purification. Samples of plantain peels were obtained from disposal outlet in Uyo metropolis, Nigeria. The peels were cut into smaller sizes, thoroughly washed first with tap water, thereafter with doubly distilled water and then oven-dried at 90˚C for 24 h. The dried samples were then ground using wooden mortar, sieved using a 100 mesh screen. The sieved fraction of the biomass was washed twice with 0.01 M HCl to remove any metal or debris that might be associated with the sample. The acid-washed samples were re-washed twice with doubly distilled water to remove acid and then further subjected to drying at a temperature of 105˚C for 12 h to obtain non-activated plantain peel (NAPP).

2.1.1. Preparation of single systems

3,7-Bis(dimethylamino)-phenothiazin-5-ium chloride, one of the commonly used dyes in the local textile industry selected as a model dye in this study was obtained from Sigma Aldrich, (Mumbai, India). A solution of 1 g/dm^3 was prepared by dissolving a quantitatively measured amount of dye into a 1 dm^{-3} volumetric flask and made up to volume with double-distilled water. Working solutions of varying concentrations were obtained by diluting the stock solution to desired concentrations. Lead, [Pb (II)], stock solution was prepared by dissolving lead carbonate ($PbCO_3$), 1.29 g in a 1 dm^{-3} volumetric flask having a solution containing 1 ml concentrated HNO_3 and made up to volume with distilled water. Concentrated HNO_3 was added to solubilize lead carbonate. Different lead concentrations were prepared from the stock solution by serial dilution.

2.1.2. Preparation of binary system

The binary system (solution) was prepared from the single solutions by physically admixing 300 ml of 1 g/dm^3 dye and metal solutions and homogenized for 10 min. Solutions of lower concentrations were subsequently prepared by serial dilution. This was properly stored as binary or multi-component solution. The contents of dye and lead in the solution were tagged as dye in mixture (DIM) and lead in mixture (LIM), respectively. This method was adopted to allow for a complete competition between adsorbate species.

2.2. Preparation and characterization of adsorbents

The activated carbon samples were obtained by both physical and chemical processes labeled as physical activated plantain peel (PAPP) and chemical activated plantain peel (CAPP), respectively, according to a reported method [31] with modifications.

(1) Physical process: A quantity of the sample in (2.1) above was placed into a stainless steel cubic reactor of dimension 20 × 2 × 2 cm and heated in a well-lagged horizontal tube furnace (model SK-G06163, China) at 5˚/min from room temperature to 650˚C and remained at this temperature for 2 h under nitrogen flow at a rate of 100 ml/min. Before heating the reactor, nitrogen was purge for about 20 min at the same rate. After carbonization, steam was supplied at rate of 50 mg/min through the carbonization bed at the same temperature for another 1 h. After the reactor was cooled to room temperature, the activated carbon was collected and washed with 0.1 M HCl to remove ash and then washed again severally with double-distilled water to remove residual acid, dried at 105˚C for 24 h to obtain PAPP.

(2) Chemical process: A quantity of the sample in (2.1) above was soaked in 100 ml 1.0 M H_2SO_4 for 12 h. Excess solution was decanted and the acid-soaked biomass was transferred into a reactor and heated as in (2.2(1) above) at 10˚/min from preheated temperature of 200 to 450˚C and remained at this temperature for 2 h under nitrogen flow at a rate of 100 ml/min. After activation, the reactor was cooled down to room temperature, the product was collected and washed with hot water repeatedly in order to remove the residual H_2SO_4 that might have been trapped in the pores until the pH of solution was between 6.5 and 7.0. Finally, the product was washed with 0.05% NaOH solution. Residual NaOH was washed out by further washing repeatedly with distilled water. The sample was then dried at 105˚C for 24 h to obtain CAPP.

2.3. Characterization of the prepared carbons

The prepared activated carbons and non-activated sample, PAPP, CAPP, and NAPP were characterized for surface area, porosity, and surface functional groups. The surface area and porosity analysis were carried out using Micromeritics Surface Area and Porosity Analyzer (Model: TriStar 3000) by nitrogen adsorption method at −196˚C after degassing all samples at 300˚C for 3 h. The surface areas and pore volumes were determined online by Tristar 3000 Analyzer program. The surface functional groups were detected using FTIR Spectrophotometer (Nicolet 6700, USA). Samples were prepared by mixing 1 mg of dried sample with 500 mg of KBr (Merck, for spectroscopy) in an agate mortar and then pressing the resulting mixture into KBR pellet under vacuum [32]. The spectra were recorded after 64 scans between 4,000 and 400 cm^{-1}. The crystal arrangement of the carbons and the composition of samples were analyzed by X-ray diffraction (XRD) (Shimadzu XRD-6000 diffractometer using Cu Kα radiation, at a scanning rate of 6˚/min with 2 ranging from 5 to 60˚).

2.4. Adsorption procedure

Adsorption was studied by batch method. Equilibrium time was optimized by running adsorption at time intervals ranging 2–60 min for individual systems and mixtures. Residual dye and metal ion concentrations were determined by UV–visible (Unicam Heλ, Model 2100, Japan) and AAS (Varian Model, AA220FS, Germany) spectrophotometers, respectively, at predetermined wavelengths (λ_{max}), (665 nm for dye) and (217 nm for Pb). The percentage adsorption for the contaminants in single system was calculated according to Eq. (1).

$$P_a(\%) = \frac{C_b - C_a}{C_b} \times 100 \quad (1)$$

where P_a is the percentage adsorption, C_b and C_a are, respectively, concentrations (mg/dm^3) of dye or metal in solution before and after adsorption. The effect of adsorbent dosage was studied by adding adsorbent (0.1–0.6 g) in 250 ml conical flasks containing 30 ml of the respective solutions at their initial pH and room temperature, and agitated mechanically for appropriate time interval after which the mixtures were filtered and residual solutions analyzed accordingly. The pH influence was monitored by adsorbing 100 mg/dm^3 of the dye and/or lead with 0.1 g of the adsorbents regulating the pH between 1 and 8 in 30 ml of solution. This range was chosen following literature reports of existence of negative charge species on the surface of agricultural waste at acidic pH, and precipitation of metals as hydroxides M $(OH)_2$ at higher pH values [33]. pH of the solutions were adjusted using 0.1 M NaOH or HCl. Initial concentration effect and isotherm study were conducted by varying the initial concentration of the dye and lead (II) from 50 to 300 mg/dm^3 at constant adsorbent weight of 0.1 g for equilibrium times corresponding to dye and lead. All experiments were conducted at room temperature (27 ± 2˚C) in a batch, agitating at a speed of 180 rpm. Adsorption capacity was calculated according to Eq. (2).

$$q_e = \frac{v}{m}(C_b - C_a) \quad (2)$$

where q_e is adsorption capacity of adsorbent (mg/g), v is the volume of adsorbate solution (mL), and m is adsorbent weight (g). Kinetics of the process was studied by running adsorption for the different solutions under constant factors but varying time interval. Experiments were also carried out for studies in binary system; adsorption capacity was calculated according to Eq. (2). It should be noted that results presented in this work are exclusive to PAPP as our drive was toward preparation and use of low-cost carbon, and also due to insignificant difference in the performance of CAPP despite having higher surface area. A similar behavior has been reported [25].

3. Results and discussion

3.1. Characterization of adsorbents

Adsorbents were prepared and characterized for surface area and porosity, and surface groups. These properties have been identified to play significant roles in the performance of real adsorbents. Carbons with improved surface area and porosity having cumulative average diameter within the micro- and meso-porosity range showed superior ability to absorb [31]. Surface area and porosity properties of the as-prepared carbons are shown in Table 1. The low-surface area of the non-activated sample is in agreement with result reported by Castro et al. [34], which the authors obtained a BET surface area of 2.0 m^2/g for banana peels, a family member of plantain, and attributed it to characteristic of non-activated carbonaceous material. The characteristic nitrogen isotherms and pore size distribution are presented in Figs. 1a and 1b. The shapes revealed the prepared carbons to be relatively mesoporous (2 nm < pore size < 50 nm) with about 77.2 and 84.4% mesopore volume on PAPP

Table 1
Textural properties of activated carbon

Adsorbent	Surface area (m^2/g)					Pore volume (cm^3/g)			Pore size (nm)	
	S_{BET}	S_{BJH}	S_{micro}	S_{ext}	$S_{t\text{-}plot}$	V_t	$V_{t\text{-}plot}$	V_{BJH}	PW_{BET}	PW_{BJH}
NAPP	1.71	0.87	0.61	1.71	1.09	0.0045	0.0003	0.0042	10.63	19.1
PAPP	177	101	105	182	72.3	0.206	0.054	0.159	4.67	7.65
CAPP	297	125	266	310	31.1	0.263	0.137	0.222	2.19	3.85

where S_{BET} is the BET surface area; S_{BJH} is the adsorption cumulative surface area of pores; and S_{micro} is the *t*-plot micropore area; $S_{t\text{-}plot}$ is the *t*-plot external surface area; and S_{ext} is the single point surface area. V_t is the total pore volume; $V_{t\text{-}plot}$ is the micropore volume; and V_{BJH} is the BJH adsorption cumulative volume of pores, PW_{BET} is the BET average adsorption pore width, and PW_{BJH} is the BET adsorption average pore diameter.

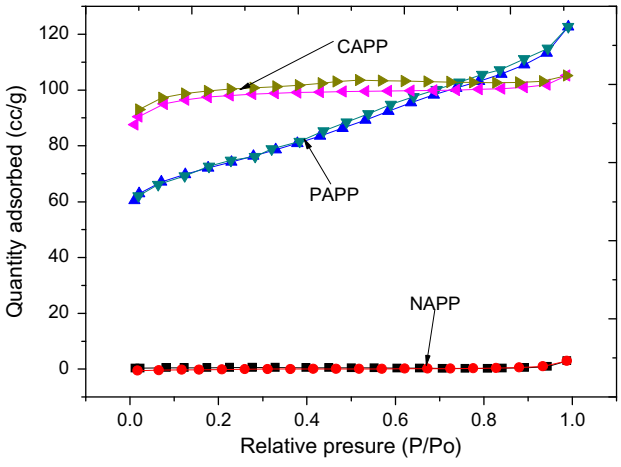

Fig. 1a. Nitrogen adsorption isotherm for prepared carbons.

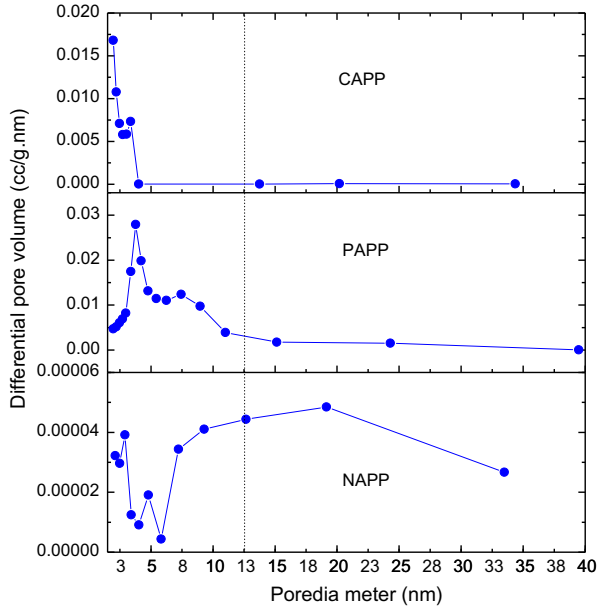

Fig. 1b. Pore size distribution of the prepared carbons.

and CAPP, respectively, with orderly distribution of pore sizes compared with non-activated peels. However, the mesopores concentrate in the lower region with small diameter 13 nm (Fig. 1b). This contributes more than 80% percent of the mesopore volume. Unlike the prepared carbons, the non-activated sample isotherm was nearly flat with no branch separating the adsorption and desorption loops, a feature of non-porous solids or solids having large macrospores [35]. In PAPP, the hysteresis loop can be observed between relative pressure ranges 0.44–1.0, indicating clearly the presence of mesopores in this carbon type. The average pore sizes given by Brunauer, Emmett, and Teller (BET) (Table 1) also confirm the porosity of the prepared carbons.

The result of XRD of the carbons is presented in Fig. 2. A relatively broad peak developed at 2θ ca. 42° is ascribed to the graphite (1 0 0) plane, while the peak (0 0 2) between 23.5 and 24° 2θ is due to the presence of carbon and graphite [36]. However, the low graphitization at the activation conditions is responsible for the amorphousness of the macroscopic carbon structure [37].

The surface functionalities of the as-prepared carbons, with the non-carbon obtained from spectra (Fig. 3) are summarized in Table 2. From the table, there is presence of saturated and unsaturated hydrocarbons, and absence of carbonyl (–C=O) and carboxylic acid (–COOH) functional groups which occur around 1,700 cm^{-1} on the non-carbon biomass surface. After activation, there is notable shift and disappearance of some functional groups from the carbon surface. This might be due to activation leading to volatilization of small molecules such as water and carbon (IV) oxide from the surface of the biomass, and transformation of one group to another (e.g. ether to carboxylic acid) on the surface of CAPP with the activating agent.

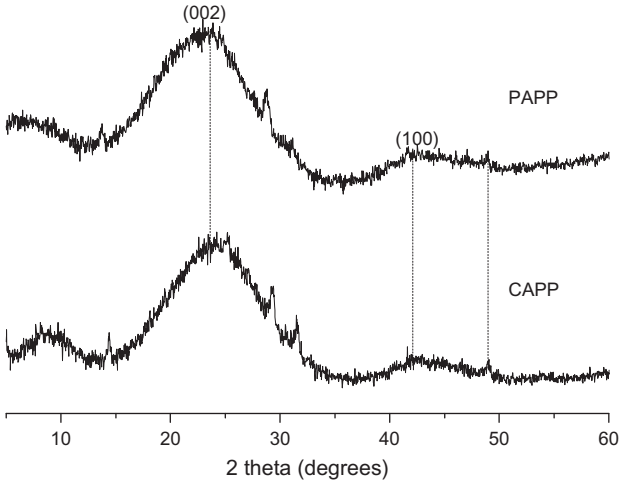

Fig. 2. XRD patterns of plantain peel activated carbons.

3.2. Effect of adsorption parameters

The adsorption capacity of agricultural waste carbon adsorbents have been reported to depend on the pH of solution, initial dye concentration, adsorbent dosage, and solution temperature [14]. The present study is focused on these factors at room temperature to understand adsorption dynamics of the individual factors.

3.2.1. Influence of pH

pH affects adsorbent's surface charge and the degree of ionization of the adsorbate [14]. Study on the effect of pH was conducted between the ranges 1–8 within error acceptability limits. The variation of percentage adsorbate uptake from solution with pH is presented (Fig. 4). In both single and binary systems, dye adsorbed maximally at pH 3.08. This is possible due to the present of negative charges on the surface of activated carbon at acidic pH due to deprotonation [38], and partly through electrostatic interaction of negative charge specie on the dye molecule. Adsorption of Pb (II) from a single solution has a pronounced effect and was favored in comparison to the dye solution. Maximum uptake was recorded between pH 4–6, after which a considerable decrease was observed; reason being that within the pH range greater surface groups deprotonation occurred. At pH greater than 8, metals in solution start to precipitate leading to reduction of metals ion in aqueous solution [32,39,40]. Hence, it is plausible to say that at higher pH values, the adsorption capacity of an adsorbent may not be relied upon as cumulative removal is a function of adsorption and precipitation. pH for maximum adsorption of LIM surprisingly occurred at around 3. This result may be caused as a result of preferential electrostatic interaction of dye molecules with the surface of adsorbent creating a surface charge for Pb (II) binding at the acidic pH and thus becoming controlling factor for Pb (II) removal. Thus, in the mixed solution, electrostatic interaction is the controlling factor subduing ionization with resultant increase in adsorption at low pH.

3.2.2. Adsorbent weight

The change in amount of carbon contacted with a given volume of both single and binary solutions with amount of solute per gram of carbon is shown in Fig. 5. Results show that adsorption capacity decreased as the adsorbent weight was increased. This means that adsorption did not increase with increase

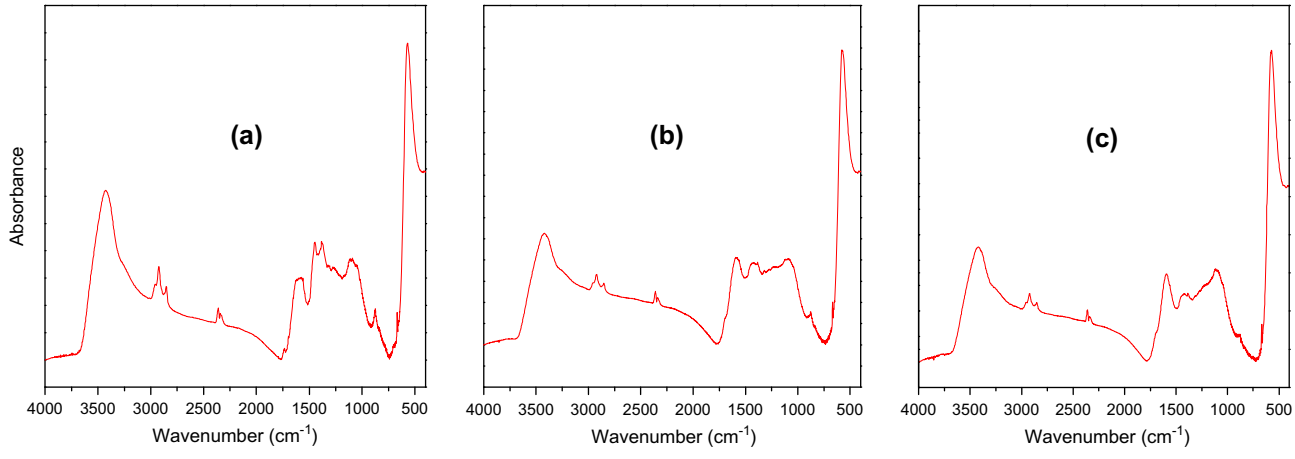

Fig. 3. FTIR spectra of (a) NAPP; (b) PAPP; and (c) CAPP.

Table 2
Surface characterization of activated carbons

Sample	V (cm^{-1})	Groups	Remarks
NAPP	569.69	–C–X	Vibration of alkylhalide (Br)
	667.66	–C–X	Stretching vibration of alkylhalide (Cl)
	875.61	–C–C	Stretching vibration of methylene group
	1,091.49	–C–O–C	Bending vibration of an ether
	1,383.49	–C–H	Bending vibrations of methyl group
	1,446.43	–C–H	Bending vibrations of methyl group C–C (in-ring) of aromatic
	1,576.23	–N–H	Strong vibration of primary amine
	2,360.69	–C≡C	Broad vibration of alkyne group
	2,923.38	–C–H, C=C	Stretching vibrations of methyl/methylene group
	3,428.75	–OH	Stretched vibration in alcohol or phenol
PAPP	577.82	–C–X	Vibration of alkylhalide (Br)
	667.40	–C–X	Stretched vibration of alkyl halide (Cl)
	1,115.8	–COOH	Stretching vibration of carboxylic group
	1,089.85	–C–O–C	Bending vibration of an ether
	1,384.56	–C–H	Bending vibrations of methyl group
	1,591.25	–N–H	Strong vibration of primary amine
	2,360.53	–C≡C	Broad vibration of alkyne group
	2,922.17	–C–H, C=C	Stretching vibrations of the methyl/methylene group
CAPP	3,422.17	–OH	Stretched vibration in alcohol or phenols
	572.46	–C–X	Vibration of alkylhalide (Br)
	667.55	–C–X	Stretching vibration of alkylhalide (Cl)
	1,114.27	–COOH	Stretching vibration of carboxylic group
	1,590.31	–N–H	Strong vibration of primary amine
	2,361.05	–C≡C	Broad vibration of alkyne group
	2,922.67	–C–H, C=C	Stretching vibrations of the methyl/methylene group
	3,423.75	–OH	Stretched vibration in alcohol or phenols

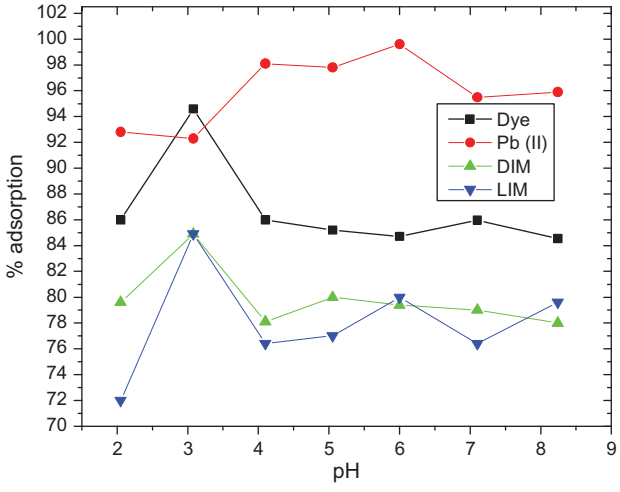

Fig. 4. Variation of percentage adsorption with pH.

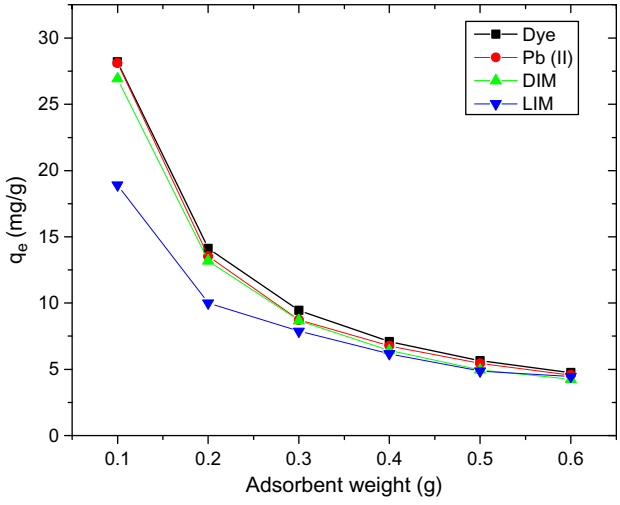

Fig. 5. Variation of adsorption capacity with adsorbent weight.

in adsorbent weight. Though an increase in adsorbent weight increases total adsorption sites, saturation of the sorption sites reached with sites corresponding to 0.1 g; and hence, no significant adsorption is observed with increased in weight. A constant number of molecules were distributed over a greater surface area leading to lower amount per unit weight.

3.2.3. Initial adsorbate concentration

The effect of initial concentration of the adsorbate solutions on the adsorbent is shown in Fig. 6. Percentage adsorption tends to increase with increase in initial concentration up to 150 mg/dm^3 and remained almost constant for higher concentrations (dye solutions), increased up to 200 mg/dm^3 for LIM and decreased for Pb (II) solution. The adsorption capacity, (q_e, mg/g), also increases with increase in initial concentration of the adsorbates. For instance, q_e increases from 13.9 to 86.9 mg/g, 12.7 to 85.9 mg/g, 9.1 to 82.3 mg/g, and 11.5 to 75.9 mg/g for dye, Pb (II), DIM, and LIM, respectively, when the initial concentration was increased from 50 to 300 mg/dm^3. This is presumably so because initial concentration provides the necessary driving force to overcome the resistance-to-mass transfer of the adsorbate ions between the aqueous and the solid phases. This trend was also noticed for adsorption in binary system but with an observable decrease in adsorption efficiency. Table 3 summaries maximum adsorption capacities of selected adsorbents for Pb (II) and dye removal in the literature. From the table, the maximum adsorption capacities obtained from our work fall within the range reported for the studied pollutants.

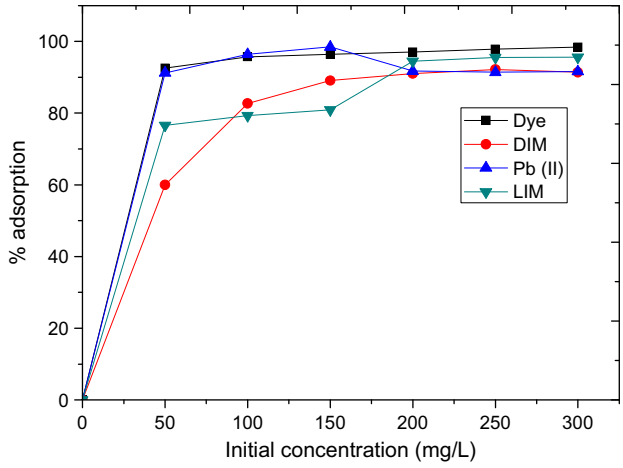

Fig. 6. Effect of initial adsorbate concentration on adsorption.

Table 3
Literature comparison of maximum removal capacity of some adsorbents (similar adsorbent species and/or metal/dye)

Adsorbents	Substrate	Maximum adsorption capacity, (q_m, mg/g)	References
Ca-modified AC	Acid Blue 25	10–110	[24]
ER-zeolite	Pb (II)	54.27	[25]
CL-zeolite		42.78	
ER-zeolite	Basic Blue 9	86.2	[25]
	Basic Voilet 3	83.80	
CL-zeolite	Basic Blue 9	77.13	
	Basic Voilet 3	70.69	
Hickory-based sorbents	Pb (II)	18.4–19.5	[27]
Cotton		69.5	
Peanut		17.7	
Hickory-based sorbents	MB	28.9–38.1	[27]
Cotton		47.9	
Peanut		49.6	
MGO	MB, OG	64.23, 20.85	[28]
Banana peels	Cu (II), Pb (II)	20.97, 41.44	[34]
Mansonia	Pb (II)	51.81	[40]
Acacia Arabica	Pb (II)	52.38	[41]
Walnut	Pb (II)	6.54	[42]
Plantain peels residue	Cr (VI)	49.93	[43]
Modified pine sawdust	Cr (VI), MB	11.86–15.78, 31.66–40.64	[44]
Succinyl grafted chitosan	Remarcyl Red TGL	193.6	[45]
Maize tasel-based carbon	Pb (II)	37.3	[46]
Persimmon tannin carbon	Pb (II)	12.4	[47]
Coconut based AC	Pb (II)	17.19–40.12	[48]
Sewage sludge-based carbon	MB	131.8	[49]
Highly porous AC	MB	48.73–185.18	[50]
Pine wood char	Pb (II)	4.13	[51]
Oak wood char		2.62	
Pine bark char		3.00	
Oak bark char		13.1	

3.3. Co-adsorption behavior of dye and metal

Adsorption of two components solution was studied to understand the effects presented by one adsorbate to another when they coexist in a system as information could be useful in selecting appropriate methods for the treatment of multi-component waste streams discharged into the environment. Visa et al. [22] reported adsorption in a binary system to be affected by two major factors which makes adsorption efficiencies to differ from those of single systems. These include: (a) ion complexation, resulting in larger volume of adsorbate specie(s), and a lower diffusion rate toward the substrate and (b) competitive adsorption between the metal ion species and the dye ion. Fig. 7 shows the relationship between equilibrium and initial adsorbate concentrations. From the figure, it is apparent the residual concentrations of dye and metal at equilibrium in the two-component system are more than in one component systems possibly due to competitive effect of the substrate ions. This means that the presence of one adsorbate in solution inhibit to an extent the sorption of the other. Sorption of lead is seen to decrease in the presence of dye (Fig. 7). The competitive effect of one adsorbate on another or the effect of dye presence on the metal or vice versa can also be evaluated using relative adsorption capacity given as:

$$q^r = \frac{q^{mix}}{q^0} \tag{3}$$

where q^r is the relative adsorption capacity, q^{mix} is the adsorption capacity of one component in the presence of the other component, and q^0 is the adsorption capacity of the same component when present alone in solution. From Eq. (3) the following conclusions can be drawn; if $q^r < 1$ adsorption is suppressed by the presence of another component, $q^r > 1$ indicates that adsorption is promoted by the presence of another component and for $q^r = 1$, the presence of more than one adsorbate has no mutual effect on adsorption of each other [40]. In this study, q^r for dye and Pb (II) are 0.708 and 0.336, respectively, both are less than unity indicating that there was suppressive interference of one component on the other during adsorption. Also q^r for dye is seen to be greater than q^r for lead meaning that the presence of lead promotes to an extent dye adsorption from the binary solution. The result in this work is in accordance with the report of Deng and his co-workers [28]. The authors found that sorption of Cd (II) onto MGO decreased in the presence of methylene blue.

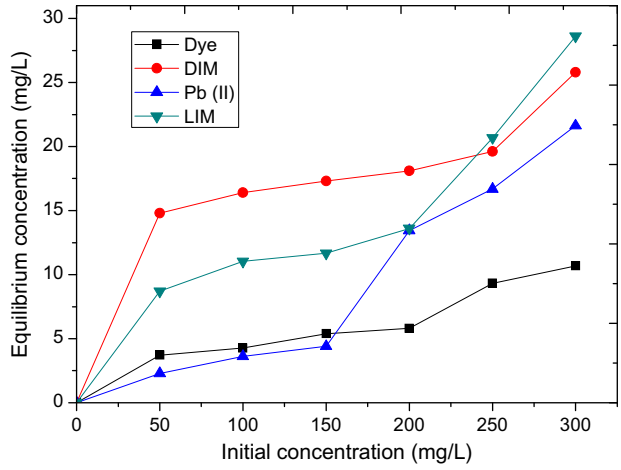

Fig. 7. Variation of initial with equilibrium adsorbate concentration.

3.4. Equilibrium isotherm

Equilibrium adsorption isotherms are usually studied to understand better the distribution of the adsorbate molecules on the surface of the adsorbent. Three isotherms: Langmuir, Freundlich, and Temkin were applied to model the single-component systems. Parametric data from the models are presented in Table 4. The Langmuir isotherm constants b (relating to energy of adsorption, L/mg) and q_o (adsorption maximum, mg/g) [52] are obtained from the slopes and intercepts, respectively, of the plots of $\frac{1}{q_e}$ against $\frac{1}{C_e}$ of the Langmuir equation (Eq. (4)).

$$\frac{1}{q_e} = \frac{1}{q_0} + \frac{1}{bC_e q_0} \tag{4}$$

where q_e and C_e are adsorption capacity and adsorbate concentration in solution at equilibrium, respectively. Eq. (5) represents the linear form of Freundlich isotherm where plots of log q_e vs. log C_e were used to obtain the Freundlich isotherm constants K_F [(mg/g)(L/g)^n], relating to adsorption capacity and n, a dimensionless constant (Table 4), which can be used to predict heterogeneity and favorability as well as type of adsorption process [53]. Freundlich isotherm assumes a heterogeneous surface with a non-uniform distribution of heat of adsorption over the surface.

Table 4
Equilibrium adsorption isotherm parameters

	Langmuir isotherm			Freundlich isotherm			Temkin isotherm		
Adsorbate	b (L/mg)	q_o (mg/g)	R^2	K_F (mg/g)(L/g)^n	n	R^2	b (J/mol)	K_T (L/g)	R^2
DYE	0.076	45.87	0.757	2.6500	0.6580	0.8985	5699.7	0.977	1.0000
Pb (II)	0.393	50.51	0.693	16.978	2.2020	0.8028	94.3	0.619	0.8992
DIM	0.032	32.47	0.445	5.6550	0.2902	0.6051	18.9	0.077	0.7996
LIM	0.128	16.95	0.374	1.0581	2.6990	0.3851	68.3	0.095	0.9280

$$\log q_e = \log K_F + \frac{1}{n}\log C_e \tag{5}$$

The Temkin isotherm in the form of Eq. (6) was also applied to determine the energy (heat) of adsorption relating to adsorbate–adsorbent interaction [54]. Its linear form is shown in Eq. (6). By plotting q_e against $\ln C_e$, values of b (J/mol) and K_T (L/g) can be calculated from the slopes and intercepts, respectively. Positive value of the constant, b (J/mol) from Temkin isotherm is an indication of an endothermic process.

$$q_e = \frac{RT}{b}\ln K_T + \frac{RT}{b}\ln C_e \tag{6}$$

Justifying from the poor correlation between the solid and liquid molecules in Table 4, it was difficult to fit experimental data to Langmuir and Freundich isotherms for single and binary component systems. Deviation in single-component system may suggest different adsorption mechanism, whereas in the mixture solution the possibility may arise from the complexities and competition of adsorption in multi-component system [3,21]. Extended Langmuir was employed to fit the experimental data.

3.4.1. Extended Langmuir isotherm modeling for binary component adsorption

In a multi-component system, there is interference and competition between the different components for adsorption sites [55]. The isotherm models for a single-component system are therefore not applicable. A multi-component system, such as binary solution, requires a mathematical isotherm model which accounts for the interactions. The multi-component systems modified Langmuir equation is given below [56,57].

$$q_{e,j} = \frac{q_j^0 b_j C_j}{1 + \sum_{k=1}^{1} b_i C_i} \tag{7}$$

where C_j is the equilibrium concentration of species j and C_i is the equilibrium concentration of all other adsorbing species in multi-component solution, while q_j^0, b_j, and b_i are constants obtained from single-component system isotherm. For this binary system, the model can be expressed as:

$$q_{e,d} = \frac{q_d^0 b_d C_{e,d}}{1 + b_d C_{e,d} + b_m C_{e,m}} \tag{8}$$

$$q_{e,m} = \frac{q_m^0 b_m C_{e,m}}{1 + b_d C_{e,d} + b_m C_{e,m}} \tag{9}$$

where the subscript, d and m represent dye and metal, respectively, in the mixed system, other terms have their usual Langmuir isotherm meanings. It should be noted that the concentrations of both pollutants in the matrix were the same and hence the study could not be described with multi-component model of the Freundlich isotherm model popularly referred to as Sheindorf–Rebuhn–Sheintuch (SRS) model [58,59].

Competition and interaction between the dye and the metal are significant and affect each component to an extent, as revealed by the relative adsorption capacity. From this model, it is assumed that Pb (II) ions are more strongly attached to the surface of the sorbent as shown by the better fit of the extended Langmuir isotherm (Fig. 8) for the metal than the dye (dye: $R^2 = 0.899$; Pb (II): $R^2 = 0.946$). However, this is not true and cannot be validated since it fails to predict fitness for both substances and confirmed by experimental data (Fig. 7) and Eq. (3).

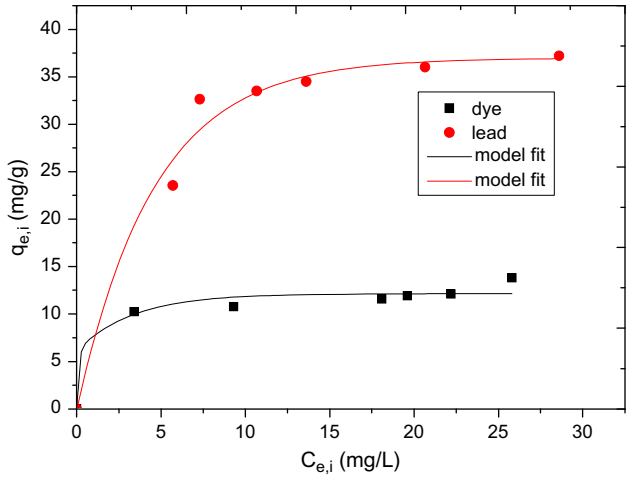

Fig. 8. Extended Langmuir isotherm for adsorption from binary system of dye and Pb (II).

3.5. Kinetics of adsorption

Pseudo-second-order kinetics of reaction fits the process more than the pseudo-first-order kinetics as shown in Table 5. Data were obtained from a plot of $\frac{1}{q_t}$ against t (Fig. 9(a)) in Eq. (10) [60]. K_2 (g/mg min) and q_e (mg/g) are pseudo-second-order rate constant of adsorption and adsorption capacity obtained from the model and can be calculated from the intercepts and slopes, respectively, of the lines in Fig. 9(a).

$$\frac{1}{q_t} = \frac{1}{k_2 q_e^2} + \frac{1}{q_e} t \tag{10}$$

The theoretical and experimental adsorption capacity values based on the pseudo-second-order kinetic are in close agreement. On the other hand, pseudo-first-order kinetics which is linearly shown in Eq. (11) poorly correlates experimental data and hence the process could not be described based on this model. In the literature, similar cases have been reported where adsorption fitted exclusively to pseudo-second-order kinetics [16,40].

$$\log (q_e - q_t) = \log q_e - \frac{K_1}{2.303} t \tag{11}$$

In Eq. (11), q_t (mg/g) and k_1 (/min) are, respectively, instantaneous adsorption capacity and pseudo-first-order kinetics rate constant. The initial sorption of the process is shown in Fig. 9(b). It is obvious from the figure that sorption at the beginning increases exponentially as the initial concentration is increased. Thus, the higher the concentration of adsorbate ions in the solution, the higher the probability of collisions between these species is, and hence the adsorbate ions could be bonded to the active sites on the surface of the adsorbent.

3.6. Mechanism of adsorption

Based on our FTIR, pH effect, and Kinetics results, adsorption is proposed to proceed through chemical reaction and electrostatic interaction of the pollutants with the surface groups (e.g. hydroxyl, carboxyl, and amine) of the carbon which provide active sites for binding. The chemical reaction is characterized by sharing of pairs of electrons (delocalized electrons on the carbon surface) between atoms of dye molecule and/or metal ion. Unlike single solution adsorption, adsorption mechanism in multi-component solution is very complex because of interactions of different types [45]. In the binary system it is proposed the negatively charged specie of the dye molecule preferentially attached to the carbon surface at acidic pH, creating a carbon-dye surface for attachment of Pb (II) ions; this may be confirmed by higher capacity of dye in the mixed solution. The summarized scheme is shown below and in Fig. 10.

$$\text{AC-OH} \rightarrow \text{AC-O}^{-}\text{H}^{+} + \text{Dye} \rightarrow \text{AC-ODye} + \text{H}^{+}$$

Dye solution system

Table 5
Adsorption kinetics parameters for the adsorption of dye and lead

		Pseudo-first-order kinetic			Pseudo-second-order kinetic		
Adsorbate	$q_{e\text{expt}}$	K_1 (/min)	$q_{e\text{cal}}$	R^2	K_2 (g/mg min)	$q_{e\text{cal}}$	R^2
DYE	28.20	0.2225	10.47	0.2189	0.2723	28.25	0.9992
Pb (II)	28.11	1.6350	3.94	0.5432	0.2246	27.47	0.9996
DIM	26.96	0.0732	6.81	0.1726	0.5068	27.55	0.9999
LIM	26.70	0.1718	2.11	0.5150	0.6984	25.51	0.9949

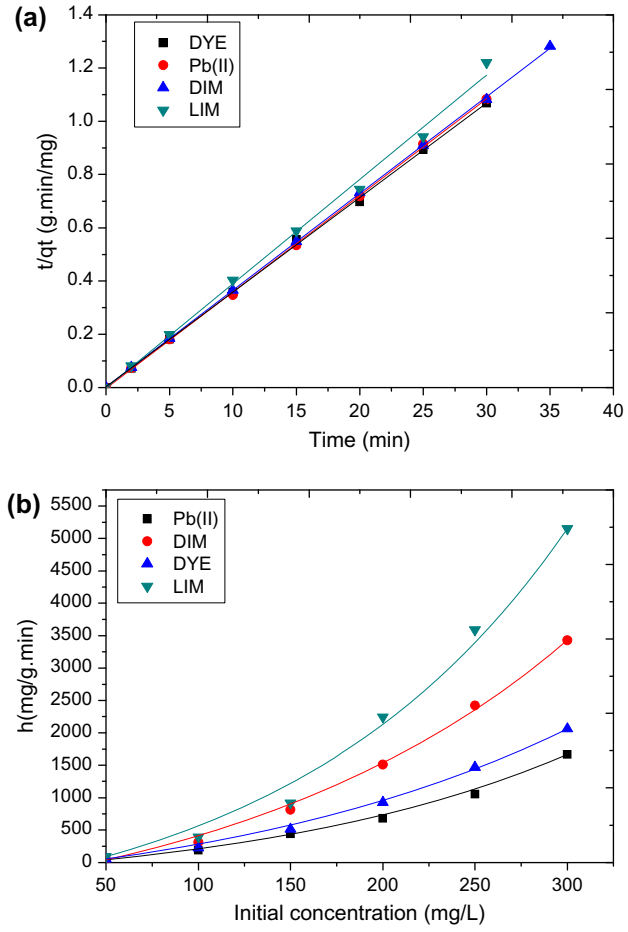

Fig. 9. (a) Pseudo-second-order kinetic model of adsorbate adsorption and (b) initial sorption rates of adsorbates onto activated carbon.

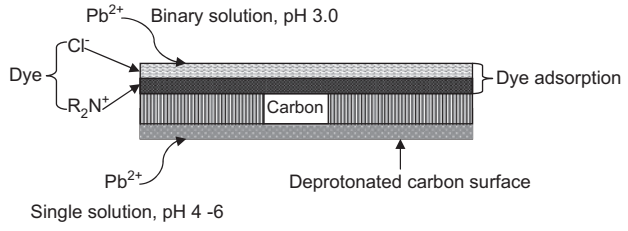

Fig. 10. Schematic representation of adsorption in single and binary solutions.

$$\text{AC-OH} \rightarrow 2\text{AC-O}^{-}\text{H}^{+} + \text{Pb}^{2+} \rightarrow (\text{AC-O})_2\text{Pb} + 2\text{H}^{+}$$

Metal solution system

$$\text{AC-OH} \rightarrow \text{AC-O}^{-}\text{H}^{+} + \text{Dye/Pb}^{2+} \rightarrow \text{AC-Dye-Pb}^{2+} + \text{H}^{+}$$

Binary solution system

4. Conclusions

Activated carbon prepared from plantain peels has potential for use as sorbent for adsorption of pollutants from textile wastewater containing mixture of dyes and heavy metals. Surface properties showed the as-prepared carbon to adsorb at the active site. High adsorption efficiency is achievable with 0.1 g of the adsorbent and in the acidic pH range. Adsorption of the pollutants was fast and attained equilibrium after about 25 min for dye and 30 min for metal. Kinetics fit extensively to pseudo-second-order kinetic model. Relative adsorption capacity for the binary process revealed antagonistic adsorption process.

Acknowledgments

The authors wish to acknowledge the members of State Key Laboratory of Heavy Oil Processing, Key Laboratory of Catalysis, China University of Petroleum, Huadong, China for use of their research facilities in preparation and characterization of the adsorbent used in this work.

References

[1] G.Z. Kyzas, M. Kostoglou, Green adsorbents for wastewaters: A critical review, Molecules 7 (2014) 333–364.
[2] T. Sismanoglu, Y. Kismir, S. Karakus, Single and binary adsorption of reactive dyes from aqueous solutions onto clinoptilolite, J. Hazard. Mater. 184 (2010) 164–169.
[3] M. Prasad, H.-Y. Xu, S. Saxena, Multi-component sorption of Pb (II), Cu (II) and Zn (II) onto low-cost mineral adsorbent, J. Hazard. Mater. 154 (2008) 221–229.
[4] T.J.K. Ideriah, O.D. David, D.N. Ogbonna, Removal of heavy metal ions in aqueous solutions using palm fruit fibre as adsorbent, J. Environ. Chem. Ecotoxicol. 4(4) (2012) 82–90.
[5] M.H. Isa, E.H. Ezechi, Z. Ahmed, S.F. Magram, S.R.M. Kutty, Boron removal by electrocoagulation and recovery, Water Res. 51 (2014) 113–123.
[6] B.K. Körbahti, K. Artut, C. Gecgel, A. Özer, Electrochemical decolorization of textile dyes and removal of metal ions from textile dye and metal ion binary mixtures, Chem. Eng. J. 173 (2011) 677–688.
[7] V.K. Gupta, Suhas, Application of low-cost adsorbents for dye removal—A review, J. Environ. Manage. 90 (2009) 2313–2342.
[8] Z. Bekci, C. Ozveri, Y. Seki, K. Yurdakoc, Sorption of malachite green on chitosan bead, J. Hazard. Mater. 154 (2008) 254–261.
[9] C.A. Basar, Applicability of the various adsorption models of three dyes adsorption onto activated carbon prepared from waste apricot, J. Hazard. Mater. 135 (2006) 232–241.
[10] N.S. Nasri, U.D. Hamza, S.N. Ismail, M.M. Ahmed, R. Mohsin, Assessment of porous carbons derived from

sustainable palm solid waste for carbon dioxide capture, J. Clean Prod. 71 (2014) 148–157.
[11] M. Hadi, M.R. Samarghandi, G. McKay, Equilibrium two-parameter isotherms of acid dyes sorption by activated carbons: Study of residual errors, Chem. Eng. J. 160 (2010) 408–416.
[12] O.F. Olorundare, R.W.M. Krause, J.O. Okonkwo, B.B. Mamba, Potential application of activated carbon from maize tassel for the removal of heavy metals in water, J. Phys. Chem. Earth 50–52 (2012) 104–110.
[13] A. Khaled, A. El Nemr, A. El-Sikaily, O. Abdelwahab, Removal of direct N Blue-106 from artificial textile dye effluent using activated carbon from orange peel: Adsorption isotherm and kinetic studies, J. Hazard. Mater. 165 (2009) 100–110.
[14] M.A.M. Salleh, D.K. Mahmoud, W.A. Karim, A. Idris, Cationic and anionic dye adsorption by agricultural solid wastes: A comprehensive review, Desalination 280 (2011) 1–13.
[15] S. Rangabhashiyam, N. Anu, N. Selvaraju, Sequestration of dye from textile industry wastewater using agricultural waste products as adsorbents. A-review, J. Environ Chem. Eng. 1 (2013) 629–641.
[16] K.Y. Foo, B.H. Hameed, Preparation, characterization and evaluation of adsorptive properties of orange peel based activated carbon via microwave induced K_2CO_3 activation, Bioresour. Technol. 104 (2012) 679–686.
[17] B.H. Hameed, A.A. Ahmad, Batch adsorption of methylene blue from aqueous solution by garlic peel, an agricultural waste biomass, J. Hazard. Mater. 164 (2009) 870–875.
[18] N.K. Amin, Removal of direct blue-106 dye from aqueous solution using new activated carbons developed from pomegranate peel: Adsorption equilibrium and kinetics, J. Hazard. Mater. 165 (2009) 52–62.
[19] I.A.W. Tan, A.L. Ahmad, B.H. Hameed, Adsorption of basic dye on high-surface-area activated carbon prepared from coconut husk: Equilibrium, kinetic and thermodynamic studies, J. Hazard. Mater. 154 (2008) 337–346.
[20] B.H. Hameed, M.I. El-KhaiarySorption kinetics and isotherm studies of a cationic dye using agricultural waste: Broad bean peels, J. Hazard. Mater. 154 (2008) 639–648.
[21] D. Mohan, K.P. Singh, Single- and multi-component adsorption of cadmium and zinc using activated carbon derived from bagasse—An agricultural waste, Water Res. 36 (2002) 2304–2318.
[22] M. Visa, C. Bogatu, A. Duta, Simultaneous adsorption of dyes and heavy metals from multicomponent solutions using fly ash, Appl. Surf. Sci. 256 (2010) 5486–5491.
[23] S.R. Shukla, R.S. Pai, Adsorption of Cu (II), Ni (II) and Zn (II) on dye loaded groundnut shells and sawdust, Sep. Purif. Technol. 43 (2005) 1–8.
[24] R. Tovar-Gómeza, M. del Rosario Moreno-Virgena, J. Moreno-Péreza, A. Bonilla-Petricioleta, V. Hernández-Montoya, C.J. Durán-Valle, Analysis of synergistic and antagonistic adsorption of heavy metals and acid blue 25 on activated carbon from ternary systems, Chem. Eng. Res. Des. 93 (2015) 755–772.
[25] V. Hernández-Montoya, M.A. Pérez-Cruz, D.I. Mendoza-Castillo, M.R. Moreno-Virgen, A. Bonilla-Petriciolet, Competitive adsorption of dyes and heavy metals on zeolitic structures, J Environ. Manage. 116 (2013) 213–221.
[26] J.-L. Gong, Y.-L. Zhang, Y. Jiang, G.-M. Zeng, Z.-H. Cui, K. Liu, C.-H. Deng, Q.-Y. Niu, J.-H. Deng, S.-Y. Huan, Continuous adsorption of Pb(II) and methylene blue by engineered graphite oxide coated sand in fixed-bed column, Appl. Surf. Sci. 330 (2015) 148–157.
[27] Z. Ding, X. Hu, A.R. Zimmerman, B. Gao, Sorption and cosorption of lead (II) and methylene blue on chemically modified biomass, Bioresour. Technol. 167 (2014) 569–573.
[28] J.-H. Deng, X.-R. Zhang, G.-M. Zeng, J.-L. Gong, Q.-Y. Niu, J. Liang, Simultaneous removal of Cd (II) and ionic dyes from aqueous solution using magnetic graphene oxide nanocomposite as an adsorbent, Chem. Eng. J. 226 (2013) 189–200.
[29] R. Tovar-Gómez, D.A. Rivera-Ramírez, V. Hernández-Montoya, A. Bonilla-Petriciolet, C.J. Durán-Valle, M.A. Montes-Moránc, Synergic adsorption in the simultaneous removal of acid blue 25 and heavy metals from water using a $Ca(PO3)_2$-modified carbon, J. Hazard Mater. 199–200 (2012) 290–300.
[30] I.A. Aguayo-Villarreal, V. Hernández-Montoya, A. Bonilla-Petriciolet, R. Tovar-Gómez, E.M. Ramírez-López, M.A. Montes-Moránc, Role of acid blue 25 dye as active site for the adsorption of Cd^{2+} and Zn^{2+} using activated carbons, Dyes Pigm. 96 (2013) 459–466.
[31] M. Asadullah, I. Jahan, M.B. Ahmed, P. Adawiyah, N.H. Malek, M.S. Rahman, Preparation of microporous activated carbon and its modification for arsenic removal from water, J. Ind. Eng. Chem. 20 (2014) 887–896.
[32] F. Ahmad, W.M.A. Daud, M.A. Ahmad, R. Radzia, Cocoa (Theobroma cacao) shell-based activated carbon by CO_2 activation in removing of Cationic dye from aqueous solution: Kinetics and equilibrium studies, Chem. Eng. Res. Des. 90 (2012) 1480–1490.
[33] V.C. Srivastava, I.D. Mall, I.M. Mishra, Removal of cadmium (II) and zinc (II) metal ions from binary aqueous solution by rice husk ash, Colloids Surf., A 312 (2008) 172–184.
[34] R.S.D. Castro, L. Caetano, G. Ferreira, P.M. Padilha, M.J. Saeki, L.F. Zara, M.A.U. Martines, G.R. Castro, Banana peel applied to the solid phase extraction of copper and lead from river water: Preconcentration of metal ions with a fruit waste, Ind. Eng. Chem. Res. 50 (2011) 3446–3451.
[35] D. Liu, P. Yuan, D.Y. Tan, H.M. Liu, T. Wang, M.D. Fan, J.X. Zhu, H.P. He, Facile preparation of hierarchically porous carbon using diatomite as both template and catalyst and methylene blue adsorption of carbon products, J. Colloid Interface Sci. 388 (2012) 176–184.
[36] C. Bouchelta, M.S. Medjram, O. Bertrand, J.-P. Bellat, Preparation and characterization of activated carbon from date stones by physical activation with steam, J. Anal. Appl. Pyrolysis 82 (2008) 70–77.
[37] L. Wang, Z. Zhang, Y. Qu, Y. Guo, Z. Wang, X. Wang, A novel route for preparation of high-performance porous carbons from hydrochars by KOH activation, Colloids Surf., A 447 (2014) 183–187.
[38] S. Dawood, T.K. Sen, Removal of anionic dye Congo red from aqueous solution by raw pine and acid-treated pine cone powder as adsorbent: Equilibrium,

thermodynamic, kinetics, mechanism and process design, Water Res. 46 (2012) 1933–1946.
[39] Y. Feng, Ji-L. Gong, G-M. Zeng, Q-Y. Niu, H-Y. Zhang, C-G. Niu, J-H. Deng, M. Yana, Adsorption of Cd (II) and Zn (II) from aqueous solutions using magnetichydroxyapatite nanoparticles as adsorbents, Chem. Eng. J. 162 (2010) 487–494.
[40] A.E. Ofomaja, E.I. Unuabonah, N.A. Oladoja, Competitive modeling for the biosorptive removal of copper and lead ions from aqueous solution by mansonia wood sawdust, Bioresour. Technol. 101 (2010) 3844–3852.
[41] A.K. Meena, K. Kadirvelu, G.K. Mishra, C. Rajagopal, P.N. Nagar, Adsorptive removal of heavy metals from aqueous solution by treated sawdust (Acacia arabica), J. Hazard. Mater. 150 (2008) 604–611.
[42] B. Yasemin, T. Zeki, Removal of heavy metals from aqueous solution by sawdust adsorption, J. Environ. Sci. 19(2) (2007) 160–166.
[43] S.O. Idowu, S.O. Oni, A.A. Adejumo, Biosorption of chromium (VI) from aqueous solution by biomass of plantain (Musa paradisiaca) peel residue, Afr. J. Med. Phys. Biomed. Eng. Sci. 3 (2011) 22–27.
[44] D. Politi, D. Sidiras, Wastewater treatment for dyes and heavy metals using modified pine sawdust as adsorbent, Procedia Eng. 42 (2012) 1969–1982.
[45] G.Z. Kyzas, P.I. Siafaka, E.G. Pavlidou, K.J. Chrissafis, D.N. Bikiaris, Synthesis and adsorption application of succinyl-grafted chitosan for the simultaneous removal of zinc and cationic dye from binary hazardous mixtures, Chem. Eng. J. 259 (2015) 438–448.
[46] M. Moyo, L. Chikazaza, B.C. Nyamunda, U. Guyo, Adsorption batch studies on the removal of pb (II) using maize tassel based activated carbon, J. Chem. (2013), doi: 10.1155/2013/508934.
[47] Y. Wang, F.Z. Wang, T. Wan, S.L. Cheng, G.Q. Xu, R. Cao, M. Gao, Enhanced adsorption of Pb (II) ions from aqueous solution by persimmon tannin-activated carbon composites, J. Wuhan Univ. Technol. Mater. Sci. Ed. 28(4) (2013) 650–657.
[48] X.L. Song, H.Y. Liu, L. Cheng, Y.X. Qu, Surface modification of coconut-based activated carbon by liquid-phase oxidation and its effects on lead ion adsorption, Desalination 255(1–3) (2010) 78–83.
[49] L.H. Liu, Y. Lin, Y.Y. Liu, H. Zhu, Q. He, Removal of methylene blue from aqueous solutions by sewage sludge based granular activated carbon: Adsorption equilibrium, kinetics, and thermodynamics, J. Chem. Eng. Data 58(8) (2013) 2248–2253.
[50] M. Ghaedi, A.M. Ghaedi, F. Abdi, M. Roosta, A. Vafaei, A. Asghari, Principal component analysis- adaptive neuro-fuzzy inference system modeling and genetic algorithm optimization of adsorption of methylene blue by activated carbon derived from Pistacia khinjuk, Ecotoxicol. Environ. Saf. 96 (2013) 110–117.
[51] D. Mohan, C.U. Pittman, M. Bricka, F. Smith, B. Yancey, J. Mohammad, P.H. Steele, M.F. Alexandre-Franco, V. Gomez-Serrano, H. Gong, Sorption of arsenic, cadmium, and lead by chars produced from fast pyrolysis of wood and bark during bio-oil production, J. Colloid Interface Sci. 310(1) (2007) 57–73.
[52] I. Langmuir, The adsorption of gases on plane surfaces of glass, mica and platinum, J. Am. Chem. Soc. 40 (1918) 1361–1403.
[53] H.M.F. Freundlich, Over the adsorption in solution. J. Phys. Chem. 57 (1906) 385–470.
[54] M.J. Temkin, V. Pyzhev, Kinetics of ammonia synthesis on promoted iron catalysts, Acta Physiochim. 12 (1940) 217–222.
[55] T.F. Hassanein, B. Koumanova, Binary mixture sorption of basic dyes onto wheat straw, Bulgarian Chem. Commun. 44(2) (2012) 131–138.
[56] A.R. Khan, T.A. Al-Bahri, A. Al-Haddad, Adsorption of phenol based organic pollutants on activated carbon from multi-component dilute aqueous solutions, Water Res. 31(8) (1997) 2102–2112.
[57] G. McKay, B. Al Duri, Prediction of multicomponent biosorption equilibrium data using empirical correlations, J. Chem. Eng. 41(1) (1989) 9–23.
[58] M. Vidal, M.J. Santos, T. Abrão, J. Rodríguez, A. Rigol, Modeling competitive metal sorption in a mineral soil, Geoderma 149 (2009) 189–198.
[59] C. Sheindorf, M. Rebhun, M. Sheintuch, A Freundlich-type multicomponent isotherm, J. Colloid Interface Sci. 1 (1981) 136–142.
[60] Y.S. Ho, G. McKay, Pseudo-second order model for sorption processes, Process Biochem. 34(5) (1999) 451–465.